Developmental Cell
Article

Rotation and Asymmetric Development of the Zebrafish Heart Requires Directed Migration of Cardiac Progenitor Cells

Kelly A. Smith,[1,2] Sonja Chocron,[1,2] Sophia von der Hardt,[3] Emma de Pater,[1,2] Alexander Soufan,[4] Jeroen Bussmann,[1] Stefan Schulte-Merker,[1] Matthias Hammerschmidt,[3] and Jeroen Bakkers[1,2,*]
[1]Hubrecht Institute for Developmental Biology and Stem Cell Research
[2]Interuniversity Cardiology Institute of the Netherlands
3584 CT Utrecht, The Netherlands
[3]Max-Planck Institute of Immunobiology, D-79108 Freiburg, Germany
[4]Heart Failure Research Center, Academic Medical Center, University of Amsterdam, 1105 AZ Amsterdam, The Netherlands
*Correspondence: j.bakkers@niob.knaw.nl
DOI 10.1016/j.devcel.2007.11.015

SUMMARY

We have used high-resolution 4D imaging of cardiac progenitor cells (CPCs) in zebrafish to investigate the earliest left-right asymmetric movements during cardiac morphogenesis. Differential migratory behavior within the heart field was observed, resulting in a rotation of the heart tube. The leftward displacement and rotation of the tube requires *hyaluronan synthase 2* expression within the CPCs. Furthermore, by reducing or ectopically activating BMP signaling or by implantation of BMP beads we could demonstrate that BMP signaling, which is asymmetrically activated in the lateral plate mesoderm and regulated by early left-right signals, is required to direct CPC migration and cardiac rotation. Together, these results support a model in which CPCs migrate toward a BMP source during development of the linear heart tube, providing a mechanism by which the left-right axis drives asymmetric development of the vertebrate heart.

INTRODUCTION

The vertebrate heart develops with a clear left-right (LR) asymmetry. Defects occurring during LR patterning of the embryonic heart result in congenital heart defects such as double-outlet-right-ventricle or transposition of the great arteries and have major consequences for heart function after birth (reviewed in Ramsdell, 2005). LR asymmetry in vertebrates is controlled by a ciliated organ such as the node in mouse and Kupffer's vesicle in zebrafish embryos (Essner et al., 2002). In this ciliated organ, a fluid flow from right to left is generated, activating a left-sided gene expression program with a central role for Nodal, a member of the TGF-β growth factor family. Other growth factors such as BMP, FGF, and SHH play important roles in the development of the ciliated organ or are required to transduce the signals from the ciliated organ to the lateral plate mesoderm (LPM) (reviewed in Raya and Izpisua Belmonte, 2006). Although the signals that regulate LR asymmetry in the embryo have been extensively studied, we still do not understand how these signals control cell and tissue morphogenesis to generate asymmetric organ development.

In the zebrafish, as in most vertebrates, the heart is the first organ to develop LR asymmetry (Stainier, 2001). Prior to the formation of the cardiac tube, several genes such as *bmp4*, *lefty1*, *lefty2*, and *pitx2* are expressed asymmetrically on the left side in the LPM in close proximity to the cardiac field and in the cardiac field itself (Chocron et al., 2007, and references therein). However, the mechanisms by which these signals control asymmetric cardiac development have not yet been identified. Prior to formation of the heart tube, cardiac progenitor cells (CPCs) located within bilateral myocardial epithelia fuse at the midline ventral to the endoderm to form a cardiac cone (Glickman and Yelon, 2002; Stainier, 2001). The cardiac cone will shape into a cone with its base on the yolk, and a model has been proposed in which the cone undergoes a telescopic extension into a linear heart tube, with central cells of the cone assembling first and giving rise to the ventricle (arterial pole) and peripheral cells giving rise to the atrium (venous pole) (see Figures S1A–S1C in the Supplemental Data available with this article online). In addition, preceding this extension, a tilting process occurs that is referred to as cardiac jogging, during which the future venous pole of the heart becomes positioned toward the left side of the body axis, while the arterial pole remains at the midline (Stainier, 2001). Although the mechanism of the leftward displacement is unclear, it is subject to early left-right patterning (Chen et al., 1997) and precedes rightward looping (Figures S1D–S1F). The analysis of zebrafish mutants defective in LR patterning demonstrated that the direction of cardiac jogging predicts the direction of looping (Chen et al., 1997).

In the current work, we investigate this asymmetric patterning of heart morphogenesis. Our data, using high-resolution 4D confocal imaging and serial sectioning in combination with 3D reconstructions, show complex cellular behaviors and provide evidence for a rotation of the cardiac cone. Studying the molecular mechanisms that might drive these processes, we find a dynamic expression of *has2* in the CPCs during the jogging process, which is required for the leftward migration of CPCs and rotation of the cone. While Has2 is a permissive factor required for CPC

migration, we find that BMP signaling is instructive for directing CPC migration during these processes, thereby providing a direct link between earlier LR patterning and morphogenesis of the heart tube.

RESULTS

The Cardiac Cone of the Zebrafish Undergoes Clockwise Rotation during Tube Formation

After fusion of the bilateral cardiac fields, CPCs move in a leftward and anterior direction, reorganizing to form the linear heart tube. To date, this movement has been simplified as a tilting and extension of the cone but is yet to be thoroughly described. To gain a more comprehensive understanding of the intercellular behavior and movements of CPCs during this stage, we performed live high-resolution confocal time-lapse recordings using the *tg(cmlc2:gfp)* line (Huang et al., 2003), which specifically expresses a nuclear GFP in developing myocardial cells, starting after fusion of the bilateral cardiac fields (Figure 1A and Movie S1). Using cell-tracking software, we tracked individual cells and measured their speed and displacement. All tracked cells showed a linear displacement toward the left and anterior axis of the embryo (n = 6 embryos), with cells moving in a coherent fashion and maintaining cellular contacts with neighboring cells. We observed, however, some variation in cellular behavior (velocity and displacement) when comparing individual tracks which appeared to correlate with the origin of cells in the initial cardiac cone. Clustering tracks into four equal sectors, based on the starting position of the cells at anterior-posterior and left-right positions (I–IV; Figure 1A), we found that the tracks of cells originating from the posterior region of the cardiac cone (sectors I and IV, red and yellow tracks in Figure 1A) were longer than tracks originating from the anterior region of the cardiac cone (sectors II and III, Figure 1A), resulting in significantly higher displacement rates for CPCs from the posterior region of the cardiac cone compared with CPCs from the anterior region ($p \leq 0.005$; Figure 1B). This was not the result of indirect migration paths, as meandering indices did not differ (Figure 1C). Furthermore, looking at the distance cells moved between the individual time points suggested that the speed at which these posterior cells move is not constant (Figure 1E). This was confirmed by measuring the speed of multiple tracks during the time-lapse imaging, demonstrating that, while anterior cells move at a constant speed, posterior cells start with a similar speed, only to accelerate to double their speed before slowing down and returning to their initial speed (Figure 1F).

Comparing the migration paths of individual cells, we further observed that, during their leftward displacement, cells derived from sectors I and IV (Figure 1A) crossed each other. This suggests that, simultaneous to leftward jogging, the cardiac cone undergoes a clockwise rotation (from a dorsal view). Tracing cells from each sector over 200 min, we determined the extent of this cardiac cone rotation as 36 ± 4 degrees (SEM, n = 6 embryos) whereas the embryonic axis itself did not rotate (Figure 1D and Movie S2). Incidentally, we also measured the angle of the tilted cone relative to the LR axis. After rotation of the cardiac cone and cardiac jogging, the tube was positioned at an angle of 36 ± 3 degrees (SEM, n = 6 embryos) relative to the LR axis, the same angle as the degree of cone rotation.

Left-Right Polarity of the Cone Is Converted into Dorsal-Ventral Polarity of the Tube

Given the clockwise rotation of the developing heart tube, we postulated that a subsequent redistribution of cells of left and right identity would occur and should be detectable. We analyzed the specific expression of *lefty2*, which demarcates the left cardiac field, in 23-somite-stage embryos (Figure 2A). Double labeling with *lefty2* and *cardiac myosin light chain 2* (*cmlc2*, a marker of cardiomyocytes) (Figures 2A and 2B) or a tropomyosin antibody (labeling all cardiomyocytes, Figures 2C and 2D) revealed that in the linear heart tube *lefty2*-expressing cells are not restricted to the left half but end up largely in the dorsal part of the tube (Figure 2C) with the exception of the outflow region (Figure 2D). 3D reconstructions of serial sections confirmed a dorsal position of *lefty2*-expressing cells in the majority of the tube with the exception of the two poles, suggesting some torsion within the tube (Figures 2E–2H and Movie S3). This change in *lefty2* expression from a strictly left-right pattern to a dorsal-ventral pattern suggests that cells derived from the left cardiac field form the dorsal part of the tube and cells from the right form the ventral part. To confirm this, we performed lineage-tracing experiments by injecting *cmlc2:*mRFP DNA in either the left or right side of embryos, labeling single cells in the cardiac field (Figures 2I and 2J). Left-labeled CPCs (n = 23) invariably ended up in the dorsal part of the linear heart tube, and right-labeled CPCs (n = 11) ended up exclusively in the ventral part of the tube, consistent with the clockwise rotation of the cone and *lefty2* expression (Figure 2K,L). Together, these results demonstrate that the initial left-right polarity of the cone becomes dorsal-ventral polarity of the later heart tube after cone rotation.

Has2 Expression in Myocardial CPCs Is Required for Cardiac Jogging

We next looked into the possible molecular mechanisms driving the leftward displacement and rotation of the cardiac field. We have previously shown that hyaluronan synthase 2 (Has2) is required for cell migration of mesodermal cells during various stages of zebrafish development (Bakkers et al., 2004). Consistent with this, specific expression of *has2* was observed in the heart during fusion of the bilateral heart fields and cardiac jogging (Figures 3A–3G). Although expression of *has2* at later stages is specific for the endocardial cushions (data not shown), we found earlier expression detectable in the myocardial lineage. This was evidenced by normal expression of *has2* observed in *cloche* mutant embryos that lack endothelial cells including the endocardium (data not shown). In addition, bilateral *has2* expression overlaps with the expression pattern of *cmlc2* (Figures 3B and 3E–3G) although not all *cmlc2*-expressing progenitor cells were positive for *has2* expression. This subpopulation of *has2*-postitve, *cmlc2*-expressing cells was more obvious after fusion of the bilateral heart fields, when *has2* expression was restricted to peripheral, future atrial regions of the myocardial cone. In accordance with this observation, double in situ hybridization (ISH) showed that *has2* is expressed in a subset of *amhc (atrial myosin heavy chain)*-expressing cells (Figure 3C), a marker gene for future atrial cells, which will undergo leftward displacement (see Introduction and Figure S1). In contrast, presumptive ventricular cells, which assemble first into a tube and remain at the midline, display little *has2* expression, as is apparent in

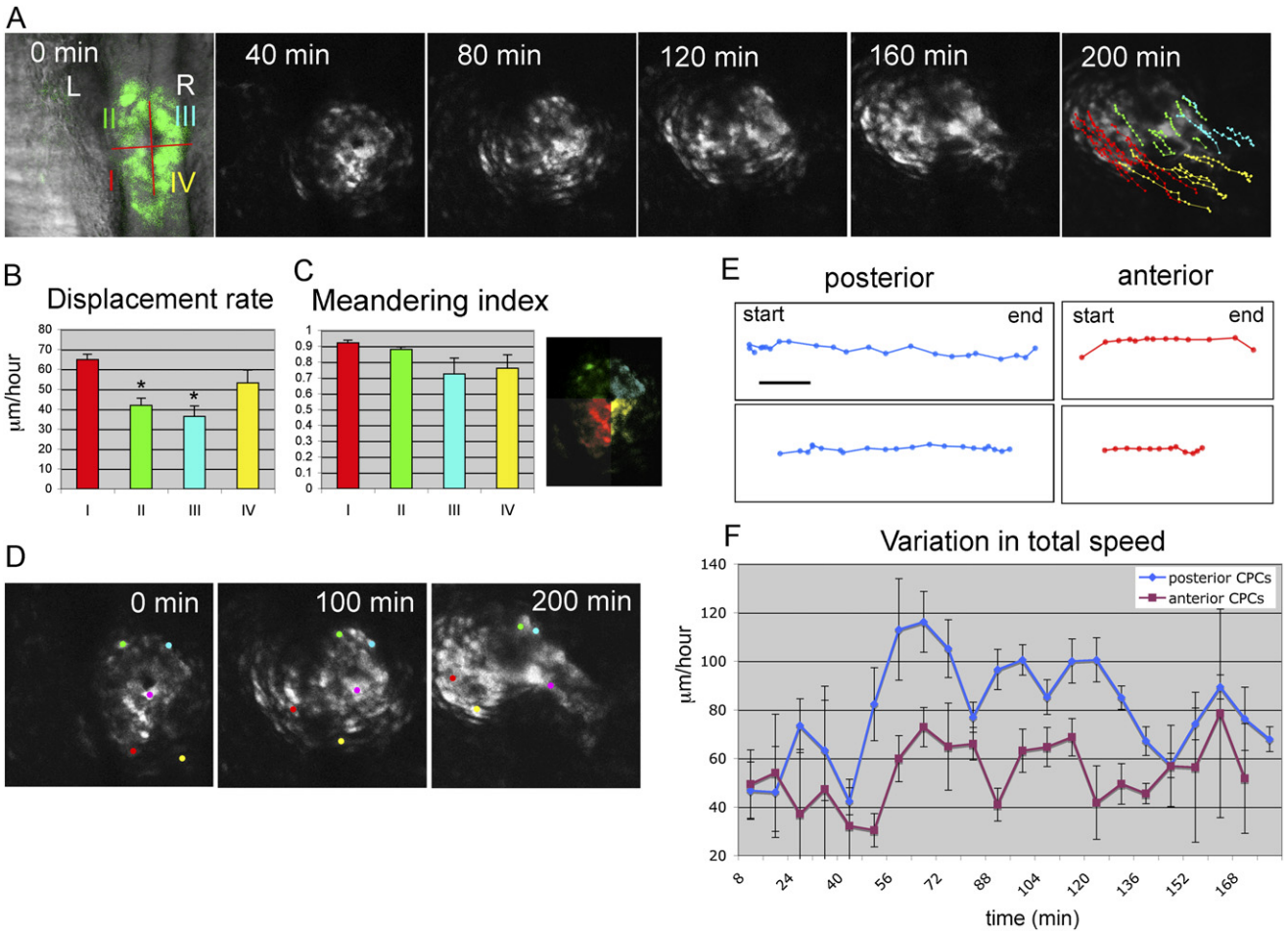

Figure 1. Rotation of the Cardiac Cone during Formation of the Linear Heart Tube

(A) Selected images of a confocal time-lapse recording of a *tg(cmlc2:gfp)* embryo starting at the 23-somite stage. Individual GFP-positive cells were tracked and color-coded according to their location within the cardiac field at the 23-somite stage. Dorsal view with anterior to the top.

(B and C) Displacement rates and meandering index (displacement/track length) of CPCs located at different positions within the cardiac field (color corresponds to position indicated in the confocal image) calculated from time-lapse recording shown in (A) (n = 30). Error bars indicate standard errors. Statistic significance (by paired t test) calculated for CPCs derived from sector I (red) compared with CPCs derived from sectors II (green) and III (blue) (* $p < 0.005$).

(D) Selected images of confocal timelapse recording with individual cells labeled during formation of the heart tube. Individual cells are marked (yellow, red, green, and blue for laterally located atrial cells and pink for medially located ventricular cells) and tracked over a 200 min period, revealing the evident rotation of the cardiac cone.

(E) Representative tracks of individual cells originating from the posterior (blue) or anterior (purple) region of the cardiac cone with 8 min intervals in between time points shown. Scale bar represents 25 µm.

(F) Graphical representation of CPC speeds during the process of heart tube formation. Cells were grouped according to their original position in the cardiac field (posterior, blue; anterior, purple).

has2 – *vmhc (ventricular myosin heavy chain)* double labeling (Figure 3D).

During the process of cardiac jogging, *has2* expression was rapidly shifted to the embryonic left side (Figures 3E and 3G) and remained restricted to the most anterior presumptive atrial cells (venous pole) of the developing heart tube. To address whether this asymmetric *has2* expression is dependent on correct LR patterning of the cardiac field, we injected a morpholino (MO) targeting the nodal related gene *southpaw* (*spaw*). *spaw* is required for correct LR patterning of the LPM, including the heart field, and injecting a MO targeting *spaw* prevents cardiac jogging (Long et al., 2003). Strikingly, we observed that in embryos injected with the *spaw* MO, *has2* expression is affected and persists in the right cardiac field (17/20 embryos) (Figures 3I and 3J).

The dynamic expression pattern of *has2* that correlates with the leftward displacement of CPCs suggests a role for Has2 in this process. In order to address whether Has2 itself is required for this displacement, we injected MOs, previously shown to specifically target *has2* (Bakkers et al., 2004). Embryos injected with *has2* MO that only mildly affect cell migration during gastrulation showed no defects in fusion of the heart fields or CPC differentiation (Figure 3H). A subtle affect on *lefty1/2* staining was observed in the heart region of *has2* morphants; however, no difference in the laterality markers, *spaw* and *pitx2*, was observed in *has2* morphants compared with control-injected embryos,

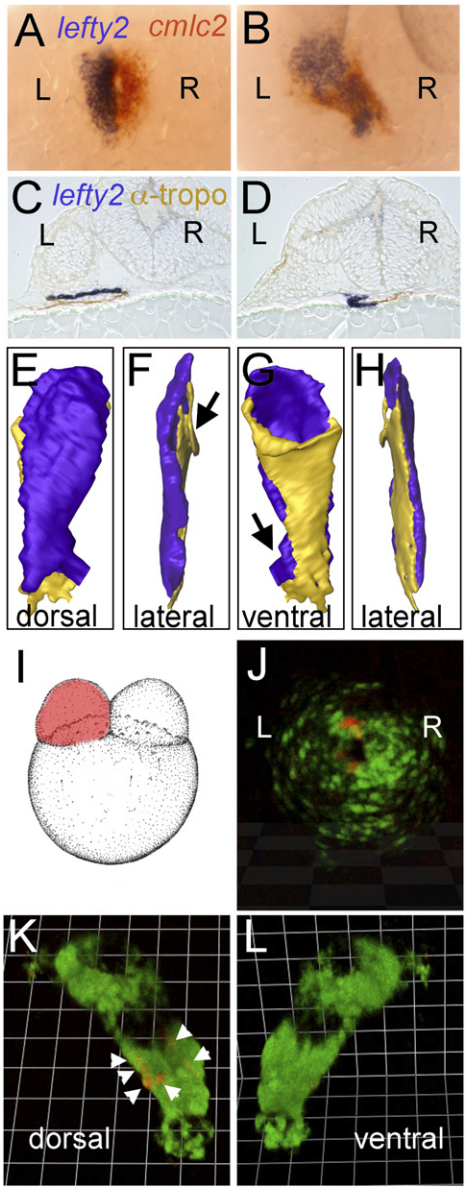

Figure 2. *lefty2* Expression and Lineage Tracing Reveals a Dorsal-Ventral Orientation of the Left-Right Regions of the Heart Field, Respectively, in the Linear Heart Tube

(A and B) Double ISH with *cmlc2* (red) and *lefty2* (blue) antisense riboprobes at 23-somite stage (A) and 24 hpf (B). Dorsal views with anterior to the top.

(C and D) Serial section and 3D reconstruction (E–H) of an ISH embryo with *lefty2* probe counterstained by using an anti-tropomyosin antibody at the level of the venous pole of the heart tube (C) and the arterial pole (D).

(E–H) 3D reconstruction with blue representing *lefty2*-positive tissue and yellow representing tropomyosin-positive tissue. (E) Dorsal view with venous pole to the top and arterial pole to the bottom. Arrows in (F) and (G) indicate regions at the poles where some torsion of the tube is visible.

(I–L) Lineage tracing of CPCs from the left or right cardiac field. (I) CPCs were mosaically labeled in the left or right cardiac field by injection of cmlc2:mRFP DNA into one cell at the two-cell stage. (J) In the cardiac cone, mRFP-expressing CPCs were observed on the left side, and these cells were later found to occupy the dorsal part (K, arrowheads) of the linear heart tube with no mRFP cells observable on the ventral side of the tube (L).

indicating that left-right patterning in these embryos was not markedly disturbed (Table S1). Thereafter, however, these embryos developed with a linear heart tube from a failure to jog toward the left side (29/55 embryos) (Figures 3K–3N). In addition, cardiac looping was severely affected in has2 MO-injected embryos (data not shown). These data suggest that Has2-dependent migration of CPCs is required as a response to early LR signals for the leftward displacement of the venous pole of the linear heart tube.

The Cardiac Cone of *has2* Morphants Fails to Rotate

To determine whether rotation of the cardiac cone was affected in conjunction with cardiac jogging in *has2* morphants, time-lapse confocal imaging and cell tracking of *tg(cmlc2:gfp)* embryos injected with *has2* MOs was performed (Figure 3O). *has2* MO injection had little effect on coherent cell movement (meandering index of 0.82 ± 0.1 SEM, n = 68). In *has2* morphants, the CPCs still migrate in linear tracks with a total speed of 50 ± 2 μm/hr (SEM, n = 68); however, there is little displacement in the left-right direction when compared with WT embryos (compare Figures 1A and 3O). In addition, cells originating from different sectors in the cardiac field all have similar displacement rates, resulting in a significant reduction in rotation of the cone ($p < 0.0005$; Figures 3P–3R and Movie S4). Remarkably, in conjunction with a failure of the cone to rotate, *lefty2*-positive cells were not found exclusively in the dorsal side of the heart tube but remain restricted to the left side (dorsal and ventral) of the heart tube in *has2* morphants (Figures 3M and 3N). It is also evident that despite the loss of rotation and leftward displacement in *has2* MO-injected embryos, the anterior displacement is only slightly delayed and a tube is still formed, albeit with a smaller lumen (Figures 3K and 3L, insets), suggesting that other forces are responsible for elongation of the linear heart tube (see also Discussion).

Activation of BMP Signaling Is Asymmetric in the LPM

Although the mechanism has not been solved, BMPs are essential for the regulation of LR asymmetry within the heart tube (Breckenridge et al., 2001; Chocron et al., 2007; Schilling et al., 1999; Zhang and Bradley, 1996). In a recent study, we were able to show a genetic interaction between Has2 and BMP signaling during dorsal convergence in the gastrulating embryo (von der Hardt et al., 2007). We observed a similar genetic interaction between Has2 and Bmp4 (the zebrafish ortholog of human BMP4) during leftward displacement of CPC (Figure S2). Prior to the initiation of cardiac jogging, *bmp4* is asymmetrically expressed in the LPM, which is regulated by earlier left-right signals including Nodal signaling (Chen et al., 1997; Chocron et al., 2007). To address whether there is asymmetric activation of BMP signaling in the LPM prior to leftward migration of the CPCs, we stained 23-somite-stage embryos with an antibody recognizing phosphorylated Smad 1,5 and 8 protein and counterstained with anti-tropomyosin antibody to label CPCs (Figure 4) and DAPI to stain all nuclei (data not shown). A confocal stack of the LPM in the region of the cardiac field detected phospho-Smad-positive cells across the LPM and surrounding the myocardium, with an asymmetric activation of phospho-Smad on the left versus right side of the embryo (Figures 4A–4C). A greater number of positive cells was observable on the

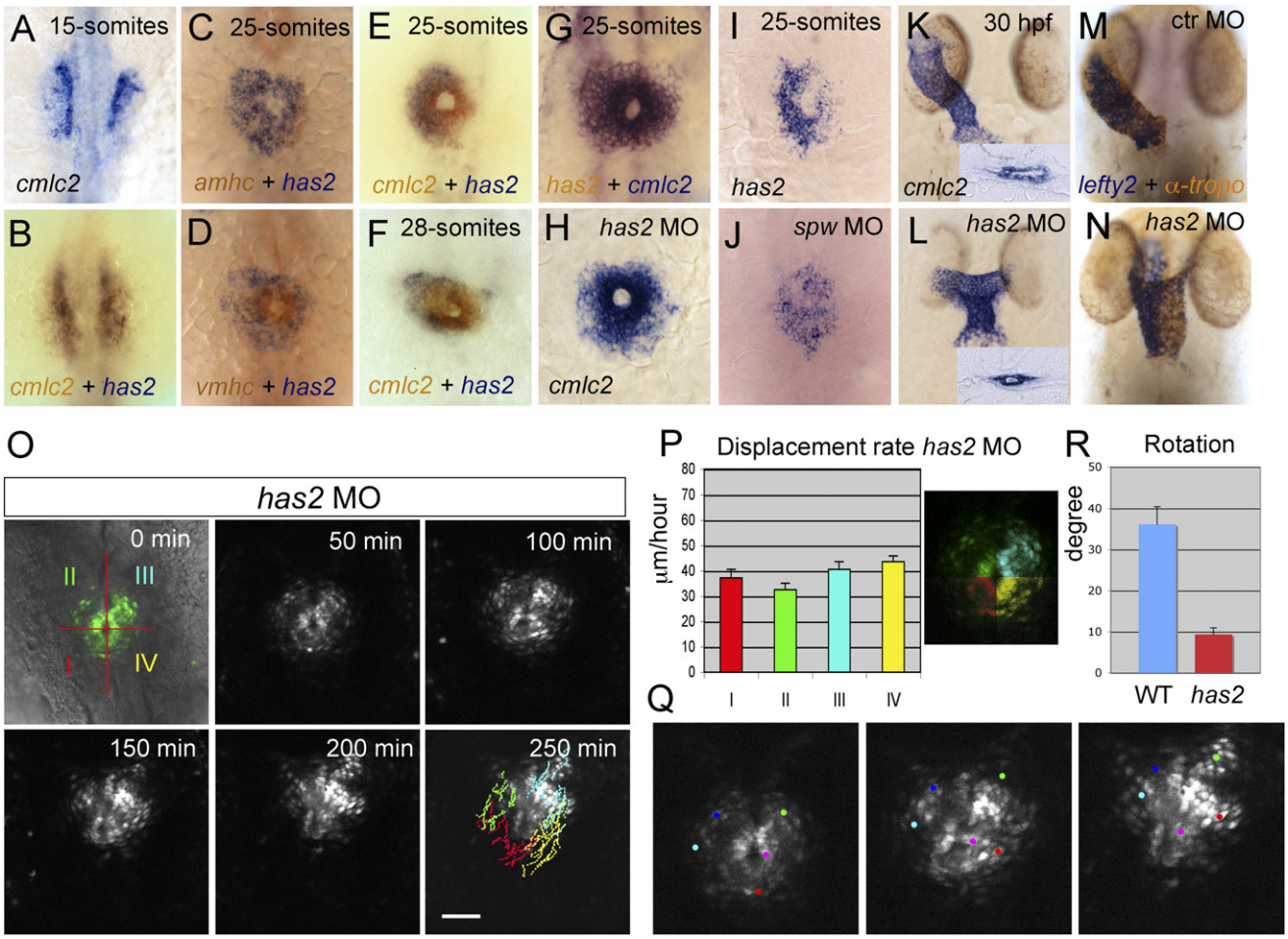

Figure 3. Has2 Expression in CPCs Is Required for Jogging and Rotation of the Cardiac Cone

(A–L) One- and two-color ISH (probes indicated at bottom) on wild-type embryos (A–G, I, and K) or embryos injected with a *southpaw* MO (J) or a *has2* MO (H and L) during various stages (indicated at the top) of heart tube formation. Evident is the dynamic expression pattern of *has2* in the CPCs. All images are dorsal views with anterior to the top and left to the left.

(M and N) Combined ISH with an antisense *lefty2* riboprobe (blue) and anti-tropomyosin antibody staining (brown, labeling all cardiomyocytes) of a control MO-injected embryo (M) or *has2* MO-injected embryo (N).

(O) Selected images of a confocal time-lapse recording of a *tg(cmlc2:gfp)* embryo injected with a *has2* MO starting at the 23-somite stage. Individual GFP-positive cells were tracked and color coded according to their location within the cardiac field at the 23-somite stage. Dorsal views with anterior to the top.

(P) Displacement rates of CPCs localized at different positions within the cardiac field (color corresponds to position indicated in the confocal image) calculated from time-lapse recording shown in (O) (n = 55, mean ± SEM). Evident is the absence of leftward displacement of the CPCs and their equal displacement rates.

(Q) Selected images of a confocal time-lapse recording shown in (O) with individual cells marked (red, light blue, dark blue, and green for atrial cells located lateral and pink for ventricular cells located medial) and tracked over a 250 min period.

(R) Quantification of clockwise cardiac cone rotation in wild-type and *has2* MO-injected embryos (mean ± SEM).

left side (Figure 4B, arrowheads) compared with the right (Figure 4B, arrows), and cell counting demonstrated this to be a statistically significant difference (Figure 4G, # $p < 0.05$, n = 6). As an additional confirmation of this patterned activation of Smad 1,5,8, we performed immunostaining in *tg(hsp70:noggin3)* embryos heat shocked at the 15-somite stage to induce Noggin expression and subsequently block BMP signaling (Chocron et al., 2007). Significantly fewer overall cells were stained for phospho-Smad 1,5,8 in these embryos (Figures 4D–4F and 4H; * $p < 0.001$, n = 5–6), and there was no significant left-right asymmetry of phospho-Smad-positive cells in *tg(hsp70:noggin3)* embryos (Figure 4I).

BMP Signaling Is Required for Directing CPC Migration

It has been well characterized that mutants with defective BMP signaling do not undergo cardiac jogging (Chen et al., 1997; Chocron et al., 2007). Given this defect, the genetic interaction of BMP signaling with Has2, and the asymmetric activation of BMP signaling in the LPM, we were interested in determining whether BMP signaling is also required for rotation of the cardiac cone. *Lost-a-fin* mutants have defective BMP signaling due to a loss-of-function mutation in the BMP type I receptor gene, *alk8* (Bauer et al., 2001; Mintzer et al., 2001). It was also apparent that *laf/alk8* mutant embryos have a smaller cardiac field at 23 somites (data not shown). Monitoring CPC movements in

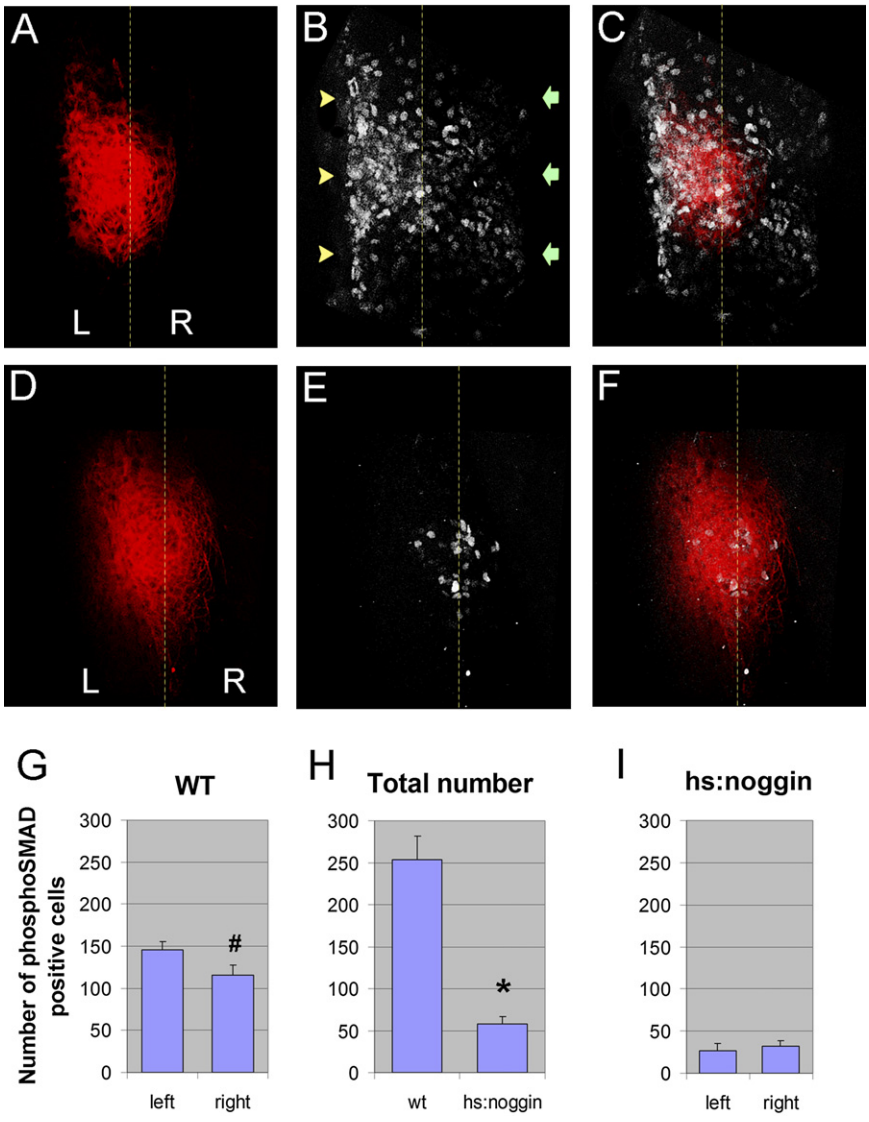

Figure 4. Asymmetric Activation of Smad 1,5,8 Protein in the LPM

Confocal images of the LPM at the cardiac region in 23-somite stage embryos stained for tropomyosin (red, A and D), phospho-Smad 1,5,8 (white, B and E), and the overlay (C and F). Staining in WT embryos (A–C) shows asymmetric activation of Smad 1,5,8 on the left side (yellow arrowheads) compared with right (green arrows). Cell counting showed this difference to be statistically significant ([G]; mean ± SEM, # $p < 0.05$). Activation of Smad 1,5,8 was significantly lower in *tg(hsp70:noggin3)* embryos (D–F) compared with WT embryos ([H]; mean ± SEM, * $p < 0.001$), and the difference between left and right activation of Smad 1,5,8 was not significant ([I]; mean ± SEM). In all images anterior is to the top, left is to the left side, and the midline is demarcated by the dashed yellow line.

laf/alk8 mutant embryos showed a reduced rotation (23 ± 10 degrees, n = 3) when compared with wild-type embryos (36 ± 4 degrees) (Figures 5A and 5D and Movie S5). The fact that this was not a complete loss of rotation may be attributed to the presence of other BMP receptors. Indeed, in *tg(hsp70:noggin3)* embryos heat shocked at the 15-somite stage, leftward displacement of the venous pole and rotation of the cardiac cone were efficiently blocked (n = 5) (Figures 5B and 5D and Movie S6). When migration paths were examined in *laf/alk8* mutant embryos, CPC movement was irregular, while in WT embryos the paths of individual CPCs were straight (Figures 6A and 6B). This difference was manifested in the meandering index of the cells (Figure 6I). Measurement of the vectors (direction of displacement) demonstrated an obvious effect on the direction of cell migration upon reduced BMP signaling. While WT CPCs coordinately migrate in an anterior-left direction, CPCs in *laf/alk8* mutant embryos migrated in an almost entirely anterior direction (Figures 6D and 6E). In addition, during their migration in the left-anterior direction, WT posterior CPCs accelerate, resulting in a much higher speed compared with the anterior cells that do not accelerate (Figures 1B and 1E and Figures 6G and 6J). This acceleration of the posterior cells is lost in *laf/alk8* mutant embryos, resulting in near-identical migration speeds for all CPCs in the cardiac field (Figure 6G). Finally, the combined reduction in total speed and the directionality of the CPC migration in *laf/alk8* mutants results in a dramatic reduction of their displacement rates (Figure 6H). These data demonstrate that BMP signaling is required for normal migration of CPCs during heart tube formation.

Given the asymmetric activation of BMP signaling in the LPM (Figure 4), we next investigated whether localized BMP signaling is required for proper CPC migration. If so, migration should not only be perturbed by loss of BMP signaling but also by uniformly high signaling levels. To test this, we utilized the previously described *tg(hsp70:bmp2b)* line in the *tg(cmlc2:gfp)* background which, upon heat shock, ectopically expresses *bmp2b* (the zebrafish ortholog of human BMP2) in the entire LPM within several hours following heat shock (Chocron et al., 2007; Scheer et al., 2002). While the heat shock alone does not affect cardiac jogging, cardiac jogging was efficiently blocked when BMP signaling was induced at the 18-somite stage or earlier (Figure 5E). Strikingly, we also observed groups of cardiomyocytes that did not incorporate normally into the heart tube, giving the tube a disheveled appearance (Figure 5E). The lack of jogging was not due to differences in cardiomyocyte specification or levels of *has2* expression, as examination of the cardiac field (by ISH for *cmlc2* or *has2*) in *tg(hsp70:noggin3)* and *tg(hsp70:bmp2b)* embryos at 23 somites revealed no differences compared with WT embryos (data not shown). When we investigated whether this lack of jogging was accompanied by a failure of the cardiac cone to rotate, we observed almost a complete absence of

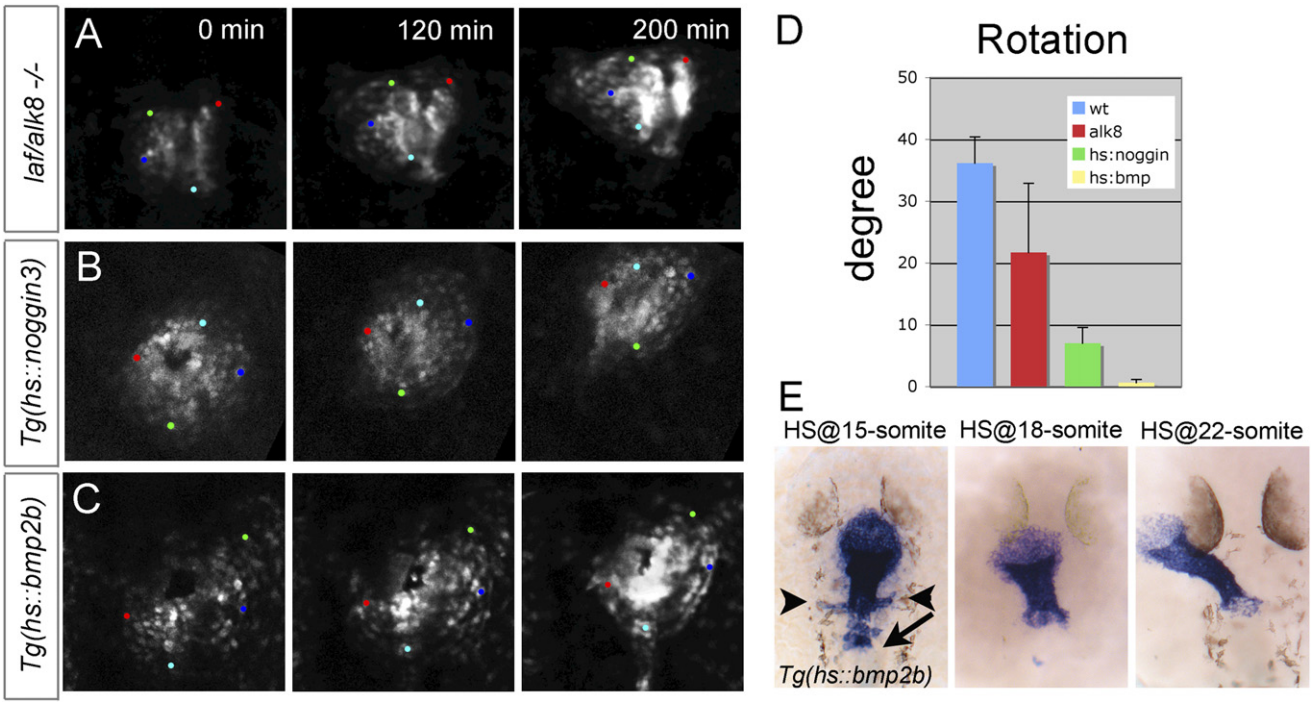

Figure 5. Leftward Displacement of CPCs and Cardiac Rotation Are Affected upon Reduced or Ectopic BMP Signaling

(A–C) Selected images of confocal time-lapse recordings of *laf/alk8* (A) heat-shock induced (at 15-somite stage) *tg(hsp70:noggin3)* (B) and *tg(hsp70:bmp2b)* (C) embryos with individual cells marked and tracked over a 200 min period.

(D) Quantification of clockwise cardiac cone rotation in wild-type *laf/alk8* mutant *tg(hsp70:noggin3)* and *tg(hsp70:bmp2b)* embryos (mean ± SEM).

(E) ISH with a *cmlc2* riboprobe on *tg(hsp70:bmp2b)* embryos heat shocked at various time points (indicated at the top). Arrows and arrowheads indicate CPCs not properly incorporated into the cardiac tube. Heat shock at 15-somite stage, no cardiac jogging (n = 14/16); 18-somite stage, no cardiac jogging (n = 12/20); 22-somite stage, leftward jogging (n = 17/19).

clockwise rotation in *tg(hsp70:bmp2b)* embryos (1 ± 1 degree, n = 3, Figures 5C and 5D and Movie S7).

Kinetic measurement of CPCs in *tg(hsp70:bmp2b)* embryos revealed that, like *laf/alk8* mutants, migration paths were obviously disturbed (Figure 6C). Measuring the vectors in *tg(hsp70:bmp2b)* embryos revealed a dramatic effect on CPC directionality that was more pronounced than that observed in *laf/alk8* mutants (Figures 6D–6F). Ectopic activation of BMP ligand resulted in CPC migration in apparently random directions. This disoriented migratory behavior is also reflected in the low meandering index for these cells (meandering index of 0.28 ± 0.02 compared with 0.86 ± 0.02 in WT embryos) (Figure 6I). Furthermore, in *laf/alk8* mutants no acceleration of the posterior cells was observed, resulting in consistent speeds between the anterior and posterior cells (Figure 6G). This combined reduction in speed and directed movement resulted in an overall significant reduction in the displacement of CPCs (Figure 6H). Altogether, these data demonstrate that BMP signaling was not only necessary but required in a localized fashion for appropriate CPC migration during heart tube formation.

BMP Beads Direct Cardiac Jogging

The acceleration of posterior CPCs during their migration suggests that these cells move toward a localized source of a chemo-attractant. The specific loss of this acceleration when BMP signaling is modulated and the asymmetric phospho-Smad distribution suggests that BMPs are likely involved in directing CPC movement. To address whether a local source of BMP ligand can direct the migration of CPCs, we implanted BMP-loaded beads into embryos. The effect of this manipulation on BMP signaling was monitored by immunostainings for phospho-Smad 1,5,8 protein. While implantation of PBS beads had no effect on the activation of Smad protein, implanting BMP beads resulted in local stimulation of Smad 1,5,8 phosphorylation (Figures 7A and 7B). The BMP beads were implanted at the 15–18-somite stage (15 hpf) in the LPM at different positions relative to the cardiac field, and cardiomyocytes were visualized by ISH after the cardiac tube was formed (28 hpf). While implanting PBS beads had no effect on CPC behavior (7/7 embryos), implanting BMP beads prevented heart tube morphogenesis when the bead was placed in direct contact with the cardiac field (data not shown). Implanting beads at a distance from the field, however, had no effect on heart tube morphogenesis. We therefore injected a *bmp4* MO to disturb endogenous BMP signaling before implanting the BMP beads in close proximity to the heart field. This resulted in various defects ranging from large parts of the heart tube covering the BMP bead to groups of cells diverging away from the cardiac field and toward the BMP bead (Figures 7C–7E).

Next, we addressed whether it was possible to redirect cardiac jogging toward a BMP bead in *bmp4* morphant embryos. BMP beads were implanted on the left or right side of *tg(cmlc2:gfp)* embryos injected with a *bmp4* MO, and cardiac jogging was visualized by time-lapse confocal microscopy. For the majority,

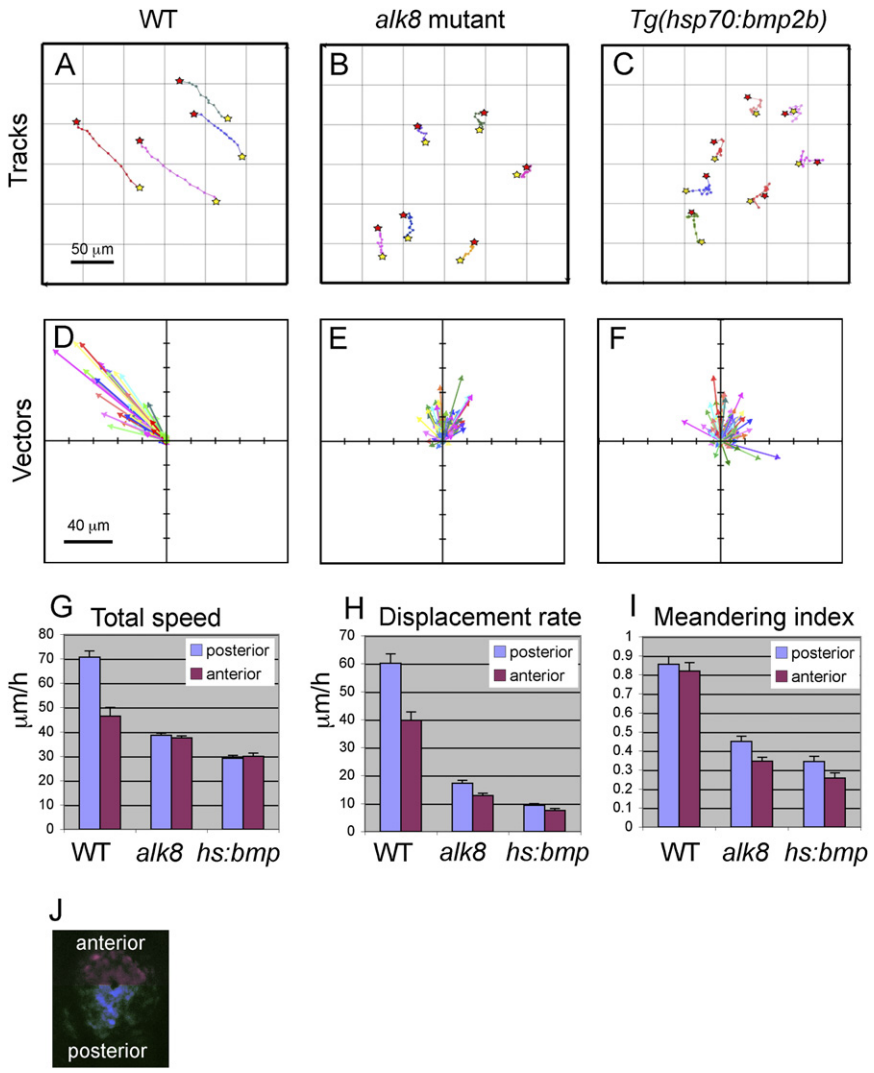

Figure 6. Coherent and Directional Migration Is Regulated by Levels of BMP Signaling

(A–C) Representative tracks from confocal time-lapse recordings over 60 min with 5 min intervals (25-somite stage). Yellow star indicates start point and red star indicates end point. Anterior to the top and left toward the left side.

(D–F) Vectors of individual cell tracks calculated from representative confocal time-lapse recordings indicating the net displacement in the anterior-posterior and left-right direction. Anterior to the top and left toward the left side.

(G–I) Graphical illustrations of the total speed and net displacement rate in μm/hr and the meandering index (displacement/track length) of CPCs in the posterior or anterior region of the cardiac field (n = 30, mean ± SEM). Evident are the reduced speed of the posterior cells and the lack of directionality when BMP signaling is modulated.

(J) Confocal image of the cardiac cone with posterior and anterior cells indicated, respectively, in blue and purple.

cardiac jogging was directed toward the BMP bead when placed either on the left (5 out of 7 embryos) or right side (11 out of 15 embryos) (Figures 7F–7G′, Movie S8). From the time-lapse movies, it was evident that cells in close proximity to the BMP bead exhibited a greater response than those at a distance, preventing an analysis of cone rotation (see also Discussion).

Finally, we investigated whether the recruitment of CPCs toward the exogenous BMP source was also Has2 dependent. We coinjected *bmp4* MO and *has2* MO in *tg(cmlc2:gfp)* embryos before implanting BMP beads on either the left or the right side. Coinjection of *has2* MO indeed prevented cardiac jogging toward the BMP source when the bead was placed on the left (6 out of 6 embryos) or right side (9 out of 13 embryos) (Figures 7H and 7H′, Movie S9). Together, these results demonstrate that local activation of BMP signaling can guide the direction of cardiac jogging and that this process requires the presence of Has2.

DISCUSSION

In zebrafish, heart tube formation from the cardiac cone has, to date, been described as an extension and elongation of this cone, in the same manner as one extends a telescope. This rather oversimplified model of what is a highly complex reorganization of the heart field has been addressed with the current work. Tracking of single cells revealed clear differences in migratory behavior of CPCs in the cardiac cone during the jogging process. This results in a simultaneous rapid leftward displacement and clockwise rotation of the cardiac cone which is Has2 dependent. In addition, we have shown that localized BMP activity regulated by early LR signaling in the LPM directs CPC migration toward the left side, uncovering a mechanism by which LR signaling controls heart morphogenesis.

Our time-lapse recordings and cell-tracking data demonstrate a dynamic and complex movement of CPCs resulting in a simultaneous coherent movement in the anterior-left direction and a clockwise rotation of the entire cardiac cone. In *has2* morphants or in embryos with reduced or ectopic BMP activity, both the rotation as well as the jogging of the cone is affected. Rotation of the heart tube is recognized in other vertebrates, including human (De la Cruz, 1998; Männer, 2000), and is described here in the zebrafish embryo. In the chick embryo, dextral looping (transformation of the linear heart tube into the c-shaped heart loop) has been described as a clockwise rotation (De la Cruz, 1998; Männer, 2000) resulting in a change of the initial left-right polarity into a dorsal-ventral polarity (Campione et al., 2001). Although various mechanisms have been suggested to drive dextral looping, there is only limited experimental data supporting this model. Recently, it was proposed by biomechanical models that rotation at the poles of the heart tube is sufficient to drive dextral looping (Männer, 2004; Voronov et al., 2004). Our results demonstrate a clockwise rotation of the zebrafish heart

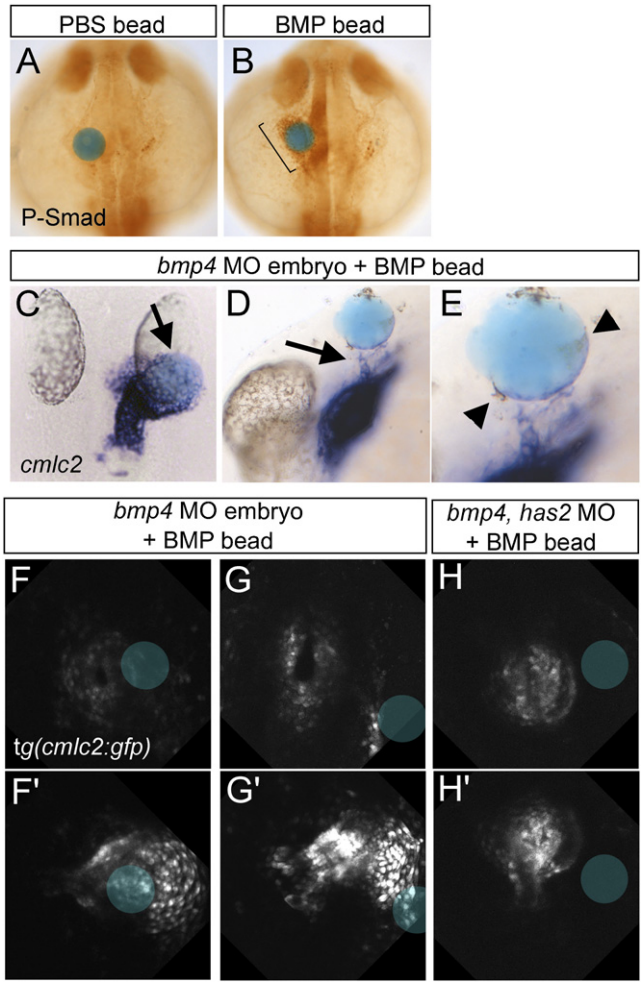

Figure 7. BMP Beads Direct Cardiac Jogging

(A and B) Phospho-Smad 1,5,8 antibody staining after implantation at the 15-somite stage of a PBS bead (A) or a BMP bead (B). Bracket in (B) indicates the induced phospho-Smad staining in close proximity of the BMP bead. Dorsal view with anterior to the top of 25-somite stage embryos.

(C–E) ISH with antisense *cmlc2* riboprobe of embryos injected with a *bmp4* MO and a BMP bead implanted at the 15–18-somite stage. (C) The heart tube is redirected to a BMP bead implanted on the right side (11/15), dorsal view with anterior to the top, arrow indicates position of the BMP bead. (D) In a lateral view, arrows indicate CPCs that have been recruited toward the BMP bead (n = 7/8). Arrowheads (E) point to a layer of CPCs that form a layer on the bead's surface. (E) is an enlargement of (D).

(F–H′) Selected images of a confocal time-lapse recording of *bmp4* morphants (F–G′) or a *bmp4 has2* double morphant (H and H′) with a BMP bead placed on the right side. Images represent the start (F–H) and end point (F′,G′,H′) of the time-lapse of the three individual embryos. Position of the BMP beads is marked by the blue circle.

cone, which is most apparent at the atrial pole, leading to a conversion of the original left and right sides to dorsal and ventral sides of the heart tube at 24 hpf. Since our analysis stopped after heart tube formation and before its dextral looping, we do not know whether this rotation continues and whether it might also be correlated to or even drive the looping of the zebrafish heart. Interestingly, however, the heart tube of *has2* morphants, as well as the heart tubes of embryos with ectopic or reduced BMP activity, fail to loop at later stages (Chen et al., 1997; Chocron et al., 2007, and J.B unpublished data). We addressed whether the clockwise rotation of the cardiac cone is reversed or simply does not occur in embryos with heart reversals such as in the embryos with a BMP bead implanted on the right side. The results were inconclusive due to the high variability in CPC movements in this artificial system. Therefore, additional forward genetic screens will be required to identify mutants that display complete heart reversals. The zebrafish provides an excellent model for future studies into the relationship between cardiac rotation and looping and the mechanisms driving these events.

During the leftward displacement and clockwise rotation, the cardiac cone also extends into a tube. Extension of the tube requires an atypical PKC and a Na,K-ATPase (Rohr et al., 2005; Shu et al., 2003). Our results demonstrate that extension of the heart tube is not dependent on Has2 activity or BMP signaling since the extension process still occurs when these pathways are affected. This would suggest that the mechanism of heart tube extension is independent of the leftward displacement and clockwise rotation of the tube. This is in agreement with our results that acceleration of a subset of CPCs is required for the leftward displacement and rotation of the heart, which is Has2- and BMP dependent. Without this acceleration of the posterior CPCs, all cells move with the same speed in the anterior direction as observed in Has2-deficient embryos (see Figure 3).

We identified Has2, which is required for cell migration in various tissues (Bakkers et al., 2004), to be specifically expressed in the CPCs of the venous pole of the heart. As seen in chick and mouse embryos, Has2 is strongly expressed in the CPCs (Klewer et al., 2006). During their migration, CPCs invade the lateral plate mesoderm, which we have shown in the current work requires Has2 in the CPCs. This is in agreement with previous reports showing that Has2 is required for migration of various cell types by a cell-autonomous mechanism (Bakkers et al., 2004; Itano et al., 2002). Has2 produces hyaluronic acid (HA), an extracellular glycosaminoglycan which has been implicated in tumor metastasis. While large polymers of HA can form a water-containing space-filling jelly, smaller oligosaccharides of HA can be bound by specific receptors, such as CD44 or Rhamm, resulting in cytoskeletal changes by activation of the small GTPases, Rho, Rac, and Ras (reviewed in Turley et al., 2002). Interestingly, cardiac-specific inhibition of Rho family proteins in mouse embryos results in reduced heart looping and poor trabeculation in the ventricle (Wei et al., 2002). Similar defects were found in mouse embryos deficient for Has2 (Camenisch et al., 2000), although direct comparison is difficult as our data did not address this later process of heart morphogenesis.

Although most studies on BMP signaling describe its effect on cell differentiation, there have been a number of reports describing chemo-attractant properties of BMP proteins on various cell types (Cunningham et al., 1992; Fiedler et al., 2002). Here, we show that CPCs can also migrate toward a source of BMP (Figure 7). This provides a direct link between the LR pathway and cardiac morphogenesis since the asymmetric *bmp4* expression in the LPM is affected in mutants with LR patterning defects (Chen et al., 1997; Chocron et al., 2007). Whether the BMP ligand itself acts as a chemo-attractant or whether BMP signaling acts more indirectly by affecting cell adhesion and/or guidance remains to be investigated. We observed an asymmetric activation

of BMP signaling in the LPM, with significantly more cells activated on the left side than the right. This patterned activation of phospho-Smad 1,5,8, which is lost in *tg(hsp70:noggin3)*, suggests that these responding cells may be instrumental in directing the rotation and the leftward displacement of the cardiac cone.

Our data demonstrate that the BMP type I receptor, Alk8, is required for guiding CPC migration. The relatively mild effect of the *laf/alk8* mutation on cardiac rotation may be explained by a redundancy with other type I receptors such as Alk3 and Alk6. The role of BMPs in directing cell migrations has recently been revealed for the dorsal convergence of mesodermal cells during gastrulation (von der Hardt et al., 2007). However, in that case, cells migrate away from the source of BMP protein, suggesting a different mode of regulation. In other vertebrates, BMPs are crucial for regulating cardiac LR asymmetry. In E8.0 mouse embryos, *Bmp2* is also expressed in the CPCs and the surrounding mesoderm (Zhang and Bradley, 1996); however, this *Bmp2* expression is symmetric without a clear difference between the right and left sides of the embryo. Possibly, since many factors such as antagonists and/or coreceptors such as heparin sulfate proteoglycans influence BMP signaling, resultant BMP signaling may still be asymmetric. Mice deficient for *Bmp2* die around E10.5 with severe cardiac defects such as a misplaced cardiac tube or, when heart tubes are present at the correct location, an unlooped tube (Zhang and Bradley, 1996; M. Mallo, personal communication). In *Xenopus* embryos, *Bmp4* is asymmetrically expressed during heart tube formation with a stronger expression on the left side (Breckenridge et al., 2001). Furthermore, ectopic expression of Noggin or a dominant-negative BMP receptor results in severe looping defects. Together, these results demonstrate that BMPs regulate asymmetric cardiac development in most vertebrate organisms studied to date. However, whether the mechanisms by which this is regulated are similar to what we have demonstrated here remains to be investigated.

To summarize, using time-lapse recordings and cell tracking we have described the dynamic and complex movement of CPCs during formation of the linear heart tube from the cardiac cone. These movements involve a simultaneous migration of CPCs in the anterior-left direction accompanied by a clockwise rotation of the entire cardiac cone. Furthermore, we have demonstrated that rotation of the zebrafish heart tube requires Has2, an enzyme involved in extracellular matrix remodeling during migration, to assist in the coordinated migration of CPCs. Finally, this migration is directed by BMPs in the lateral plate mesoderm. This complex reorganization that takes place to establish the linear heart tube may also have implications on later patterning of the heart.

EXPERIMENTAL PROCEDURES

Fish Lines and Heat-Shock Experiments

Fish were kept under standard conditions as previously described (Westerfield, 1995). *Lost-a-fin/alk8* mutant allele used in this study is *laf* ^{tm110b} (Mullins et al., 1996). The *tg(cmlc2:gfp)*, *tg(hsp70:noggin3)*, and *tg(hsp70:bmp2b)* lines were previously described (Chocron et al., 2007; Huang et al., 2003). Heat-shock experiments were performed as described previously (Chocron et al., 2007).

Morpholino Injections

Morpholino oligonucleotides (MOs; Gene Tools) were dissolved in water to 1 mM. For injection (1 nl per embryo), MOs were diluted in 1x Danieu's buffer (Nasevicius and Ekker, 2000). All morpholinos used have been described previously; *has2* MO (Bakkers et al., 2004), *bmp4* MO (Chocron et al., 2007), *spaw* MO (Long et al., 2003).

Lineage Tracing

Cmlc2:mRFP in pCS2 was injected into one cell at the two-cell stage into *tg(cmlc2:gfp)* embryos at a concentration of 20 ng/μl (1 nl per embryo). Embryos were screened for mosaic mRFP fluorescence on the right or left side exclusively and imaged at 20 somites and 28 hpf by confocal imaging.

ISH, Immunohistochemistry, and Sectioning

ISH was carried out as previously described (Westerfield, 1995). Embryos were cleared in methanol and mounted in benzylbenzoaat/benzylalcohol (2:1) before pictures were taken. Embryos were mounted in Technovit 8100 (Hereaus Kulzer) and sectioned at 3 μm thickness. 3D reconstructions of serial sections were performed as described before (Soufan et al., 2003). Immunohistochemistry was performed as previously described (Dong et al., 2007). Mouse anti-Tropomyosin (Sigma) and rabbit anti-phospho-Smad (Cell Signaling) were applied at 1:200.

Time-Lapse Imaging and Analysis

Embryos at the 22-somite stage were dechorionated and mounted in glass-bottom 6-well plates using 0.25% agarose in E3 embryo medium containing 16 mg/ml 3-amino benzoic acid ethylester to block contractile movements. Confocal imaging was performed using a Leica SP2 confocal laser scanning microscope with 40x magnification, acquiring stacks every 5 min. Embryos were kept at 28.5°C during recordings. ImageJ software (http://rsb.info.nih.gov/ij/) was used to generate time-lapse movies and for cell counting. Automated cell tracking in 3D was done using Volocity software (Improvision) followed by manual inspection of individual tracks generating quantification of total speed (track length/time), displacement rate (displacement/time), and meandering index (displacement/track length). Rotation was calculated by measuring the angle with the LR axis of four imaginary lines connecting four individual cells at the start and the end of the time-lapse (200 min). All statistical analyses were performed in Excel (Microsoft).

Bead Implantations

Agarose beads (Affigel blue, BioRad) were rinsed twice in PBS and incubated for 1 hr at 37°C with 100 ng/μl recombinant human BMP4 and BMP7 (R&D Systems) essentially as described before (von der Hardt et al., 2007).

Supplemental Data

Supplemental Data include two figures, one table, and nine movies and can be found with this article online at http://www.developmentalcell.com/cgi/content/full/14/2/287/DC1/.

ACKNOWLEDGMENTS

We are grateful to D. Stainier and H.-J. Tsai for providing the *tg(cmlc2:gfp)* fish, J. Kuipers and M. Camacho for technical assistance, D. Yelon, J. Yost, and S. Abdelilah-Seyfried for sending plasmids, and A. Moorman and B. Hogan for critical reading of the manuscript and stimulating discussions. Work in J.B.'s laboratory was supported by the KNAW, by EU FP6 grant LSHM-CT-2005-018833, by NWO (ALW Grant #814.02.007), and by HFSP (Research Grant RGP9/2003). K.S. was supported by ICIN grant #39.740. J. Bussmann has been supported by a Boehringer Ingelheim Fonds PhD Scholarship.

Received: July 6, 2007
Revised: October 23, 2007
Accepted: November 16, 2007
Published: February 11, 2008

REFERENCES

Bakkers, J., Kramer, C., Pothof, J., Quaedvlieg, N., Spaink, H.P., and Hammerschmidt, M. (2004). Has2 is required upstream of Rac1 to govern dorsal migration of lateral cells during zebrafish gastrulation. Development *131*, 525–537.

Bauer, H., Lele, Z., Rauch, G.J., Geisler, R., and Hammerschmidt, M. (2001). The type I serine/threonine kinase receptor Alk8/Lost-a-fin is required for Bmp2b/7 signal transduction during dorsalventral patterning of the zebrafish embryo. Development *128*, 849–858.

Breckenridge, R.A., Mohun, T.J., and Amaya, E. (2001). A Role for BMP Signalling in Heart Looping Morphogenesis in Xenopus. Dev. Biol. *232*, 191–203.

Camenisch, T.D., Spicer, A.P., Brehm-Gibson, T., Beisterfeldt, J., Augustine, M.L., Calabro, A., Jr., Kubalak, S., Klewer, S.E., and McDonald, J. (2000). Disruption of hyaluronan synthase-2 abrogates normal cardiac morphogenesis and hyaluronan-mediated transformation of epithelium to mesenchyme. J. Clin. Invest. *106*, 349–360.

Campione, M., Ros, M.A., Icardo, J.M., Piedra, M.E., Christoffels, V.M., Schwieckert, A., Blum, M., Franco, D., and Moorman, A.F. (2001). Pitx2 expression defines a left cardiac lineage of cells: evidence for atrial and ventricular molecular isomerism in the iv/iv mice. Dev. Biol. *231*, 252–264.

Chen, J.N., van Eeden, F.J., Warren, K.S., Chin, A., Nusslein-Volhard, C., Haffter, P., and Fishman, M.C. (1997). Left-right pattern of cardiac Bmp4 may drive asymmetry of the heart in zebrafish. Development *124*, 4373–4382.

Chocron, S., Verhoeven, M.C., Rentzsch, F., Hammerschmidt, M., and Bakkers, J. (2007). Zebrafish Bmp4 regulates left-right asymmetry at two distinct developmental time points. Dev. Biol. *305*, 577–588.

Cunningham, N.S., Paralkar, V., and Reddi, A.H. (1992). Osteogenin and recombinant bone morphogenetic protein 2B are chemotactic for human monocytes and stimulate transforming growth factor beta1 mRNA expression. Proc. Natl. Acad. Sci. USA *89*, 11740–11744.

De la Cruz, M.V. (1998). Torsion and looping of the cardiac tube and primitive cardiac segments, Anatomical manifestations. In Living Morphogenesis of the Heart, M.V. De la Cruz and R.R. Markwald, eds. (Boston: Birkhauser), pp. 99–119.

Dong, P.D.S., Munson, C.A., Norton, W., Crosnier, C., Pan, X., Gong, Z., Neumann, C.J., and Stainier, D.Y.R. (2007). Fgf10 regulates hepatopancreatic ductal system patterning and differentiation. Nat. Genet. *39*, 397–402.

Essner, J.J., Vogan, K.J., Wagner, M.K., Tabin, C.J., and Yost, H.J. (2002). Conserved functions for embryonic nodal cilia. Nature *418*, 37–38.

Fiedler, J., Roderer, G., Gunther, K.P., and Brenner, R.E. (2002). BMP-2, BMP-4, and PDGF-bb stimulate chemotactic migration of primary human mesenchymal progenitor cells. J. Cell. Biochem. *87*, 305–312.

Glickman, N.S., and Yelon, D. (2002). Cardiac development in zebrafish; coordination of form and function. Semin. Cell Dev. Biol. *13*, 507–513.

Huang, C.J., Tu, C.T., Hsiao, C.D., Hsieh, F.J., and Tsai, H.J. (2003). Germ-line transmission of a myocardium-specific GFP transgene reveals critical regulatory elements in the cardiac myosin light chain 2 promoter of zebrafish. Dev. Dyn. *228*, 30–40.

Itano, N., Atsumi, F., Sawai, T., Yamada, Y., Miyaishi, O., Senga, T., Hamaguchi, M., and Kimata, K. (2002). Abnormal accumulation of hyaluronan matrix diminishes contact inhibition of cell growth and promotes cell migration. Proc. Natl. Acad. Sci. USA *99*, 3609–3614.

Klewer, S.E., Yatskievych, T., Pogreba, K., Stevens, M.V., Antin, P.B., and Camenisch, T. (2006). Has2 expression in heart forming regions is independent of BMP signaling. Gene Expr. Patterns *6*, 462–470.

Long, S., Ahmad, N., and Rebagliati, M. (2003). The zebrafish nodal-related gene southpaw is required for visceral and diencephalic left-right asymmetry. Development *130*, 2303–2316.

Männer, J. (2000). Cradiac looping in the chick embryo: a morphological review with special reference to terminological and biomechanical aspects of the looping process. Anat. Rec. *259*, 248–262.

Männer, J. (2004). On rotation, torsion, lateralization and handedness of the embryonic heart loop: new insights from a simulation model for the heart loop of chick embryos. Anat. Rec. *278A*, 481–492.

Mintzer, K.A., Lee, M.A., Runke, G., Trout, J., Whitman, M., and Mullins, M.C. (2001). lost-a-fin encodes a type I BMP receptor, Alk8, acting maternally and zygotically in dorsoventral pattern formation. Development *128*, 859–869.

Mullins, M.C., Hammerschmidt, M., Kane, D.A., Odenthal, J., Brand, M., vanEeden, F.M., Furutani-Seiki, M., Granato, M., Haffter, P., Heisenberg, C.P., et al. (1996). Genes establishing dorsoventral pattern formation in the zebrafish embryo: the ventral specifying genes. Development *123*, 81–93.

Nasevicius, A., and Ekker, S.C. (2000). Effective targeted gene 'knockdown' in zebrafish. Nat. Genet. *26*, 216–220.

Ramsdell, A.F. (2005). Left–right asymmetry and congenital cardiac defects: Getting to the heart of the matter in vertebrate left–right axis determination. Dev. Biol. *288*, 1–20.

Raya, A., and Izpisua Belmonte, J.C. (2006). Left–right asymmetry in the vertebrate embryo: from early information to higher-level integration. Nat. Rev. Genet. *7*, 283–293.

Rohr, S., Bit-Avragim, N., and Abdelilah-Seyfried, S. (2005). Heart and soul/PRKCi and nagie oko/Mpp5 regulate myocardial coherence and remodeling during cardiac morphogenesis. Development *133*, 107–115.

Scheer, N., Riedl, I., Warren, J.T., Kuwada, J.Y., and Campos-Ortega, J.A. (2002). A quantitative analysis of the kinetics of Gal4 activator and effector gene expression in the zebrafish. Mech. Dev. *112*, 9–14.

Schilling, T.F., Concordet, J., and Ingham, P.W. (1999). Regulation of left-right asymmetries in the zebrafish by Shh and Bmp4. Dev. Biol. *210*, 277–287.

Shu, X., Cheng, K., Patel, N., Chen, F., Joseph, E., Tsai, H.J., and Chen, J.-N. (2003). Na,K-ATPase is essential for embryonic heart development in the zebrafish. Development *130*, 6165–6173.

Soufan, A.T., Ruijter, J.M., van den Hoff, M.J.B., de Boer, P.A.J., Hagoort, J., and Moorman, A.F.M. (2003). Three-dimensional reconstruction of gene expression patterns during cardiac development. Physiol. Genomics *13*, 187–195.

Stainier, D.Y. (2001). Zebrafish genetics and vertebrate heart formation. Nat. Rev. Genet. *2*, 39–48.

Turley, E.A., Noble, P.W., and Bourguignon, L.Y.W. (2002). Signaling properties of hyaluronan receptors. J. Biol. Chem. *277*, 4589–4592.

von der Hardt, S., Bakkers, J., Inbal, A., Carvalho, L., Solnica Krezel, L., Heisenberg, C.P., and Hammerschmidt, M. (2007). The Bmp gradient of the zebrafish gastrula guides migrating lateral cells by regulating Ca2+-dependent cell adhesiveness. Curr. Biol. *17*, 475–487.

Voronov, D.A., Alford, P.W., Xu, G., and Taber, L.A. (2004). The role of mechanical forces in dextral rotation during cardiac looping in the chick embryo. Dev. Biol. *272*, 339–350.

Wei, L., Imanaka-Yoshida, K., Wang, L., Zhan, S., Schneider, M.D., DeMayo, F.J., and Schwartz, R.J. (2002). Inhibition of Rho family GTPases by Rho GDP dissociation inhibitor disrupts cardiac morphogenesis and inhibits cardiomyocyte proliferation. Development *129*, 1705–1714.

Westerfield, M. (1995). The Zebrafish Book (Oregon: University of Oregon Press).

Zhang, H., and Bradley, A. (1996). Mice deficient for BMP2 are nonviable and have defects in amnion/chorion and cardiac development. Development *122*, 2977–2986.